NUMERICAL STUDY OF MHD CONVECTIVE NANOFLUID FLOWS WITHIN A CORRUGATED TRAPEZOIDAL ENCLOSURE

Victor M. Job[1], Sreedhara Rao Gunakala[2*],

P.V.S.N. Murthy[3], R. Panneer Selvam[4]

[1,2]Department of Mathematics and Statistics, The University of the West Indies, Trinidad
[3]Department of Civil Engineering, University of Arkansas, U.S.A.
[4]Department of Mathematics, Indian Institute of Technology Kharagpur, India
[1]Email: victor.job@sta.uwi.edu
[2]Email: sreedhara.rao@sta.uwi.edu*(Corresponding author)
[3]Email: pvsnm@maths.iitkgp.ac.in
[4]Email: rps@uark.edu

Abstract*:* We consider the unsteady magnetohydrodynamic (MHD) natural convection flows of alumina (Al_2O_3)-water and single-walled carbon nanotube (SWCNT)-water nanofluids within a symmetrical corrugated trapezoidal enclosure with the effects of viscous and Joule dissipations. In this study, the corrugated bottom wall is isothermally heated, whereas the top wall is thermally insulated. The temperature of the side walls is fixed at the initial nanofluid temperature within the enclosure. We solve the governing equations for velocity and temperature, along with the corresponding initial and boundary conditions, using the polynomial pressure projection stabilized (PPPS) finite element method. The effects of sidewall inclination angle φ and Eckert number Ec on nanofluid flow and convective heat transfer within the corrugated enclosure are examined. The results obtained from this study are important in various fields of engineering and technology, such as the design and manufacture of efficient heat exchangers and the cooling of microelectromechanical systems (MEMS) using nanofluids.

Keywords: *Corrugated trapezoidal enclosure, finite element method, MHD, nanofluids, natural convection.*

https://doi.org/10.47412/OYSH8586

1. Introduction

In order to gain a better understanding of buoyancy-driven fluid flow problems in enclosures with different types of geometries, an extensive amount of research has been conducted in the past decade. Natural convection flows in enclosures with flat walls have been studied by researchers such as Khanafer and Chamkha [1], Chamkha [2], Muthtamilselvan [3], Karimipour et al. [4] and Kalaoka and Witayangkurn [5]. However, in practical problems, enclosures are often non-rectangular [6]. Therefore, the study of free (natural) convection flows in non-rectangular enclosures is important.

The understanding of free convection flows within trapezoidal enclosures is useful for the design and operation of heat exchangers or solar collectors [6,7]. Applications of trapezoidal geometries may also be found in the study of fluid flows and heat transfer in microchannels and the cooling of micro-

electromechanical (MEMS) systems [7-9]. However, the performance of these heat transfer systems is often limited by the low thermal conductivities of conventional fluids such as water, oil and ethylene glycol (EG). In this view, the use of nanofluids has been identified as an innovative method of heat transfer enhancement.

The natural convection flow of carbon nanotube-EG-water nanofluid within a trapezoidal enclosure was studied by Esfe et al. [10]. In their study, the side walls of the enclosure are insulated, whereas the bottom and top walls are maintained at a constant hot and cold temperature respectively. It was found that at low Rayleigh number, the average Nusselt number decreases when the sidewall inclination angle increases. However, for high Rayleigh number, the average Nusselt number attains a maximum value when the inclination angle is 30°. Al-Weheibi et al. [7] investigated unsteady free convection in a trapezoidal enclosure filled with nanofluids. The nanofluids considered in their study are copper, cobalt or alumina nanoparticle suspensions in water, engine oil or kerosene. The results showed that the heat transfer rate increases with increased solid volume fraction. Furthermore, for each value of the Rayleigh number, a critical value of the aspect ratio exists at which the rate of heat transfer is maximum. Akbarzadeh and Fardi [11] conducted a numerical study of natural convection flows of Al_2O_3-water nanofluid in 2D and 3D trapezoidal enclosures. It was observed that for both types of enclosures, heat transfer is enhanced by increasing the Rayleigh number. The average Nusselt number decreases when the nanoparticle volume fraction is increased from 0% to 2%, and this trend is reversed when the nanoparticle volume fraction is further increased to 4%.

Unsteady MHD free convection flows of alumina-water and SWCNT-water nanofluids within a wavy trapezoidal enclosure were studied by Job and Gunakala [12]. The authors found that the flow circulation intensity is higher in the alumina-water nanofluid than the SWCNT-water nanofluid. However, the heat transfer rate is higher in the case of the SWCNT-water nanofluid. The study also showed that an increase in nanoparticle concentration causes heat transfer enhancement for the SCWNT-water nanofluid, but reduces heat transfer for the alumina-water nanofluid. Job et al. [13] considered the effects of Rayleigh number and Hartmann number on unsteady MHD free convection alumina-water and SWCNT-water nanofluid flows within a corrugated trapezoidal enclosure. It was observed that the rate of heat transfer is decreased with enhanced natural convection. Furthermore, in the case of the SWCNT-water nanofluid, the rate of heat transfer increases with increased Hartmann number. For the alumina-water nanofluid, the heat transfer rate decreases as the Hartmann number increases through small values. However, as the Hartmann number increases through large values, the heat transfer rate increases.

In the studies conducted by Job and Gunakala [12] and Job et al. [13], the effects of sidewall inclination angle and Eckert number on unsteady convective heat transfer within a nanofluid-filled corrugated trapezoidal enclosure have not been considered. Therefore, in the present work, we investigate the influence of these parameters on flow and heat transfer phenomena in alumina-water and SWCNT-water nanofluids.

2. Mathematical Formulation

Consider the unsteady laminar and incompressible two-dimensional nanofluid flow within the trapezoidal enclosure that is depicted in Fig. 1. The height of this enclosure and the length of its top wall are both equal to h, and the left and right walls are each inclined at angle φ from the $\hat{y}$-axis. The corrugated bottom wall has length $h(1+2tan\varphi)$, amplitude $h/10$ and period $h(1+2tan\varphi)/3$. The sinusoidal geometry of this wall is described by the following equation:

$$f(\hat{x},\varphi)=\frac{h}{10}\left\{1+cos\left[\frac{6\pi(\hat{x}+htan\varphi)}{h(1+2tan\varphi)}+\pi\right]\right\}, \qquad -htan\varphi \le \hat{x} \le h(1+tan\varphi). \tag{1}$$

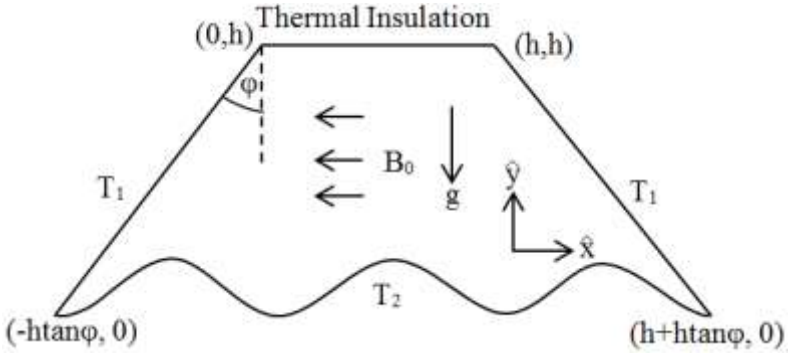

Figure 2: Schematic Diagram of the Problem

The initial temperature of the nanofluid (at $\hat{t} = 0$) is T_1. For time $\hat{t} > 0$, the temperature of the bottom wall is increased to T_2 (where $T_2 > T_1$) by a heated object located below the enclosure. The temperature at the left and right walls of the enclosure is fixed at the initial temperature T_1, whereas the top wall is thermally insulated so that heat transfer through this wall is insignificant. Temperature differences within the enclosure induce fluid flow through free convection effects, and this flow is influenced by a uniform horizontal magnetic field with flux density B_0. In this study, we assume that the magnetic Reynolds number is very small, and the electric force induced by the applied magnetic field is negligible. Viscous and Joule dissipations, which are caused by the induced fluid flow and the applied magnetic field, also influence the temperature of the fluid within the enclosure. In the absence of thermal radiation, the dimensionless governing equations for a single-phase Newtonian nanofluid are as follows [12,13]:

$$\frac{\partial u}{\partial x}+\frac{\partial v}{\partial y}=0 \tag{2}$$

$$\frac{\partial u}{\partial t}+u\frac{\partial u}{\partial x}+v\frac{\partial u}{\partial y}=-\frac{\rho_f}{\rho_{nf}}\frac{\partial p}{\partial x}+Pr\,\frac{\mu_{nf}}{\mu_f}\frac{\rho_f}{\rho_{nf}}\left(\frac{\partial^2 u}{\partial x^2}+\frac{\partial^2 u}{\partial y^2}\right) \tag{3}$$

$$\frac{\partial v}{\partial t}+u\frac{\partial v}{\partial x}+v\frac{\partial v}{\partial y}=-\frac{\rho_f}{\rho_{nf}}\frac{\partial p}{\partial y}+Pr\,\frac{\mu_{nf}}{\mu_f}\frac{\rho_f}{\rho_{nf}}\left(\frac{\partial^2 v}{\partial x^2}+\frac{\partial^2 v}{\partial y^2}\right)-Ha^2Pr\,\frac{\sigma_{nf}}{\sigma_f}\frac{\rho_f}{\rho_{nf}}v+RaPr\,\frac{(\rho\beta)_{nf}}{(\rho\beta)_f}\frac{\rho_f}{\rho_{nf}}T \tag{4}$$

$$\begin{aligned}\frac{\partial T}{\partial t}+u\frac{\partial T}{\partial x}+v\frac{\partial T}{\partial y}=\;&\frac{\kappa_{nf}}{\kappa_f}\frac{\rho_f c_f}{(\rho c)_{nf}}\left(\frac{\partial^2 T}{\partial x^2}+\frac{\partial^2 T}{\partial y^2}\right)+Ha^2Ec\,\frac{\sigma_{nf}}{\sigma_f}\frac{\rho_f c_f}{(\rho c)_{nf}}v^2\\&+Ec\,\frac{\mu_{nf}}{\mu_f}\frac{\rho_f c_f}{(\rho c)_{nf}}\left[2\left(\frac{\partial u}{\partial x}\right)^2+2\left(\frac{\partial v}{\partial y}\right)^2+\left(\frac{\partial u}{\partial y}+\frac{\partial v}{\partial x}\right)^2\right]\end{aligned} \tag{5}$$

where $Pr=\frac{\mu_f c_f}{\kappa_f}$ is the Prandtl number, $Ra=\frac{\rho_f^2\beta_f g(T_2-T_1)h^3Pr}{\mu_f^2}$ is the Rayleigh number, $Ha=B_0h\sqrt{\frac{\sigma_f}{\mu_f}}$ is the Hartmann number and $Ec=\frac{\mu_f\kappa_f}{(\rho_f c_f)^2(T_2-T_1)h^2}$ is the Eckert number. The subscripts 'f' and 'nf' indicate that a given property belongs to the base fluid and nanofluid respectively.

Equations (2)-(5) are obtained using the dimensionless variables below:

$$(\hat{x},\hat{y})=\frac{(x,y)}{h},(\hat{u},\hat{v})=\frac{\rho_f c_f h}{\kappa_f}(u,v),\hat{p}=\frac{\rho_f c_f^2 h^2}{\kappa_f^2}p,\hat{T}=\frac{T-T_1}{T_2-T_1}. \tag{6}$$

We describe the thermophysical properties of dilute nanofluids [14] using the following equations:

1. Density:
$$\rho_{nf} = (1-\phi)\rho_f + \phi\rho_s \tag{7}$$
2. Heat Capacity:
$$(\rho c)_{nf} = (1-\phi)\rho_f c_f + \phi\rho_s c_s \tag{8}$$
3. Thermal Expansion Coefficient:
$$(\rho\beta)_{nf} = (1-\phi)\rho_f\beta_f + \phi\rho_s\beta_s \tag{9}$$
4. Viscosity (Brinkman):
$$\mu_{nf} = \frac{\mu_f}{(1-\phi)^{2.5}} \tag{10}$$
5. Thermal Conductivity (Maxwell-Garnett):
$$\kappa_{nf} = \frac{\kappa_s+2\kappa_f+2\phi(\kappa_s-\kappa_f)}{\kappa_s+2\kappa_f-\phi(\kappa_s-\kappa_f)}\kappa_f \tag{11}$$
6. Electrical Conductivity (Maxwell):
$$\sigma_{nf} = \sigma_f\left[1+\frac{3(\sigma_s/\sigma_f-1)\phi}{(\sigma_s/\sigma_f+2)-(\sigma_s/\sigma_f-1)\phi}\right] \tag{12}$$

In Eqs. (7)-(12), the subscript 's' indicates that the given property belongs to the solid nanoparticle. The thermophysical properties of pure water, Al_2O_3 and SWCNTs [15-18] at $25°C$ are given in Table 1.

Table 15: Thermophysical Properties of Pure Water, $\boldsymbol{Al_2O_3}$ and SWCNTs at $\boldsymbol{25°C}$

Quantity	Pure Water	Al_2O_3	SWCNT
$\rho(kgm^{-3})$	997.1	3970	2600
$c\ (Jkg^{-1}K^{-1})$	4179	765	425
$\kappa\ (Wm^{-1}K^{-1})$	0.613	40	6600
$\beta\ (\times 10^{-5}K^{-1})$	21	0.85	0.16
$\sigma\ (\Omega^{-1}m^{-1})$	0.05	1×10^{-10}	4.8×10^{7}

From the no-slip condition, the velocity of the fluid on the boundary of the enclosure is zero. Hence, the dimensionless initial and boundary conditions for the problem are
$$u = v = T = 0 \text{ at } t = 0 \tag{13}$$
$$u = v = 0, T = 1 \text{ on the bottom wall} \tag{14}$$
$$u = v = T = 0 \text{ on the left and right walls} \tag{15}$$
$$u = v = 0, \frac{\partial T}{\partial y} = 0 \text{ on the top wall} \tag{16}$$
The average (dimensionless) Nusselt number on the corrugated bottom wall Γ of the enclosure is given by
$$Nu_{av} = \frac{1}{l(\Gamma)}\int_{\Gamma}\frac{\partial T}{\partial \boldsymbol{n}}dl, \tag{27}$$
where $l(\Gamma)$ is the length of Γ and $\boldsymbol{n}$ is the unit outward normal vector to Γ.

3. Numerical Method

The coupled system of nonlinear partial differential equations given in Eqs. (2)-(5) and the associated initial and boundary conditions (13)-(16) are solved numerically using the PPPS finite element method [19]. First, the problem is spatially discretized into three-noded linear triangular elements and a stabilized mixed Galerkin formulation is constructed. Then, the resulting system of ordinary differential equations is

discretized in time using the Crank-Nicholson scheme. This gives a system of nonlinear algebraic equations, which is solved in MATLAB using the fixed point iteration method with a relative error tolerance of 10^{-6}.

4. Grid-Independence Test and Validation of Numerical Algorithm

We conducted a grid-independence test with 50 time steps for five different uniform grids containing 5547, 6386, 7136, 8148 and 9445 elements. The numerical solution for each grid was represented by the average Nusselt number Nu_{av} on the corrugated bottom wall. The effect of the number of elements on Nu_{av} in the case of the Al_2O_3-water nanofluid at time $t = 1$ with $Pr = 6.2$ (water), $Ra = Ha = 100$, $Ec = 10^{-5}$ and $\phi = 0.02$ is shown in Table 2. We found that the relative error between values of Nu_{av} for 8148 and 9445 elements is less than 0.5%. Hence, upon consideration of the accuracy of the numerical solution and the associated computational time, we determined that a finite element grid with 8148 elements is appropriate for the present study.

Table 2: Grid Independence Test Values for $\boldsymbol{Pr = 6.2}$ (water), $\boldsymbol{Ra = Ha = 100}$, $\boldsymbol{Ec = 10^{-5}}$ and $\boldsymbol{\phi = 0.02}$

Number of Elements	Computational Time(s)	Nu_{av}	Relative Error (%)
5547	2109	4.4474	5.45
6386	2758	4.6899	1.54
7136	3006	4.7621	0.63
8148	3120	4.7322	0.47
9445	6034	4.7100	----------

The MATLAB code used for the numerical solution of the problem is validated against the benchmark solution of De Vahl Davis [20] for natural convection of air ($Pr = 0.71$) within a square enclosure with differentially-heated side walls. We compared the average Nusselt number Nu_{av} on the hot wall, maximum horizontal velocity u_{max} and maximum vertical velocity v_{max} with the work of De Vahl Davis for $Ra = 10^3$ and $Ra = 10^4$ as shown in Table 3. We found that the present code is in excellent agreement with this benchmark solution; therefore, the numerical results obtained in the present study are validated.

Table 3: Comparison of Nu_{av}, u_{max} and v_{max} from the Present Code with the Benchmark Solution of De Vahl Davis

		Present Work	De Vahl Davis [20]	Error (%)
$Ra = 10^3$	Nu_{av}	1.1178	1.118	0.01
	u_{max}	3.6469	3.649	0.05
	v_{max}	3.7098	3.697	0.34
$Ra = 10^4$	Nu_{av}	2.2529	2.243	0.44
	u_{max}	16.2633	16.178	0.52
	v_{max}	19.7991	19.617	0.93

5. Results and Discussion

Numerical results were computed at time $t = 1$ for different values of the sidewall inclination angle and Eckert number, whereas the Prandtl number, Rayleigh number, Hartmann number and volume fraction are fixed at 6.2, 100, 100 and 0.02 respectively. The effect of side wall inclination angle φ on the fluid flow and heat transfer for the two nanofluids near steady state (at $t = 1$) are shown in Figs. 2-5. It was observed

in these figures that for each of these nanofluids, the heat transfer and the strength of the flow circulation within the enclosure are directly proportional to the sidewall inclination angle. As φ increases, the length of the heated bottom wall is also increased. This results in an enhancement of heat transfer (Figs. 4 and 5) within the enclosure, and through the effects of natural convection the flow circulation intensity increases. It can be seen in Figs. 2 and 3 that the core of each primary circulation cell moves upward within the enclosure as φ increases; this upward motion is associated with an enhancement of the buoyancy force on the nanofluid with increased φ. It was also noted that the secondary circulation cells decrease in size when φ is increased. These observations may be explained by a reduction in the amplitude-to-wavelength ratio of the corrugated bottom wall as φ is increased.

The effects of the Eckert number Ec on the alumina-water nanofluid flow and heat transfer near steady state are displayed in Figs. 6 and 7. It is revealed in these figures that heat transfer and the strength of the flow circulation within the enclosure increase with increased Ec. As Ec increases, viscous and Joule dissipation effects within the fluid are enhanced; this results in an increase in temperature within the enclosure. Through the effects of free convection, the induced flow velocity within the enclosure also increases. It is noted that for lower values of Ec ($Ec \leq 10^{-5}$), heat is transferred from the hot bottom wall to the adiabatic top wall and the isotherms near to the cold side walls are almost parallel to these walls. However, for higher values of Ec ($Ec > 10^{-5}$), the heat generated due to the motion of fluid within the enclosure causes the fluid near the adiabatic top wall to attain a higher temperature than the fluid near the bottom wall. Hence, as seen in Fig. 6, heat is transferred from the top wall to the bottom wall for higher values of Ec. Fig. 7 shows that the isotherms near to the side walls are increasingly non-linear as Ec increases. This may be explained by an increase in flow intensity with increasing Ec, which enhances thermal advection within the enclosure.

Tables 4 and 5 show the average Nusselt number at the wavy bottom wall for different values of φ and Ec. It is noted that for both nanofluids, the average rate of heat transfer increases as φ increases from 0° to 45°, but decreases as φ is increased from 45° to 60°. For the alumina-water nanofluid, Nu_{av} has an inverse relationship with Ec. This indicates that as viscous and Joule dissipations increase, the rate of heat transfer within the alumina-water nanofluid is reduced. However, due to the weak flow circulation in the SWCNT-water nanofluid, there is no significant change in Nu_{av} as Ec is varied.

$\varphi = 0°$

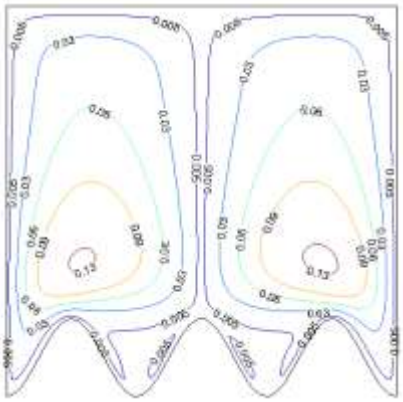

$\varphi = 0°$

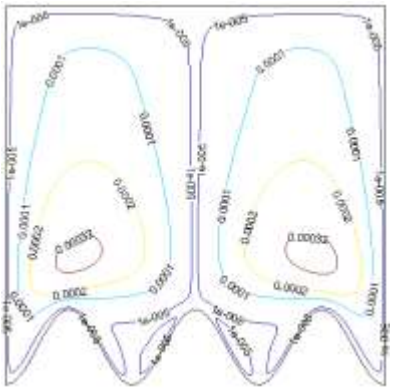

$\varphi = 45°$

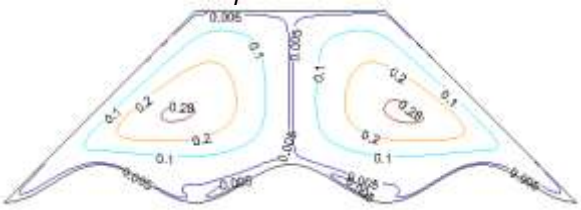

$\varphi = 60°$

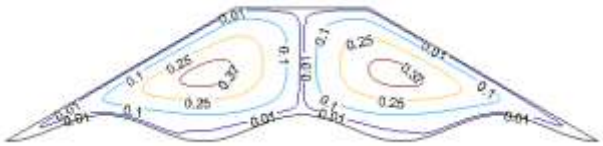

Figure 2: Streamline Plots for Different Values of φ with $Ec = 10^{-5}$ (Al_2O_3-Water Nanofluid)

$\varphi = 45°$

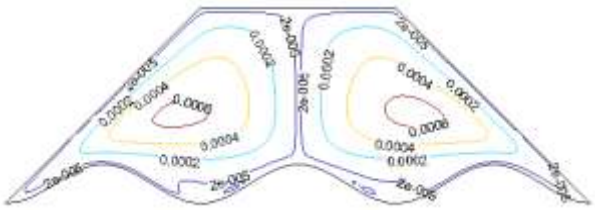

$\varphi = 60°$

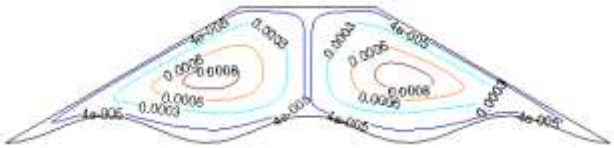

Figure 3: Streamline Plots for Different Values of φ with $Ec = 10^{-5}$ (SWCNT-Water Nanofluid)

Table 4: Average Nusselt Number for Different Values of φ with $\boldsymbol{Ec = 10^{-5}}$

φ	Nu_{av} (Al_2O_3-Water Nanofluid)	Nu_{av} (SWCNT-Water Nanofluid)
0°	3.6793	3.7411
20°	3.7336	3.8105
45°	4.7322	5.0947
55°	4.4979	4.8750
60°	4.3438	4.7946

$\varphi = 0°$

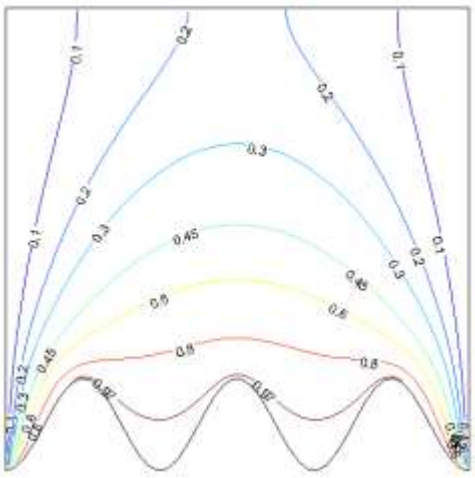

$\varphi = 45°$

$\varphi = 0°$

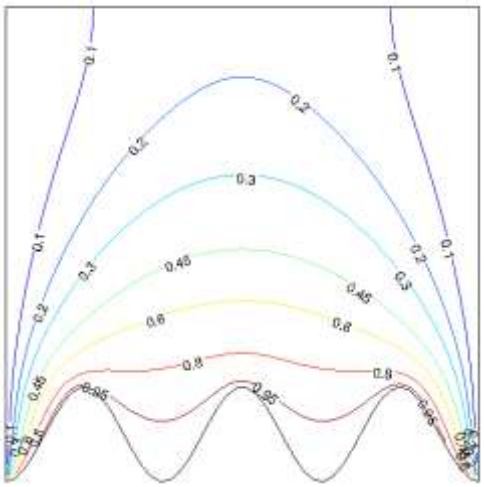

$\varphi = 45°$

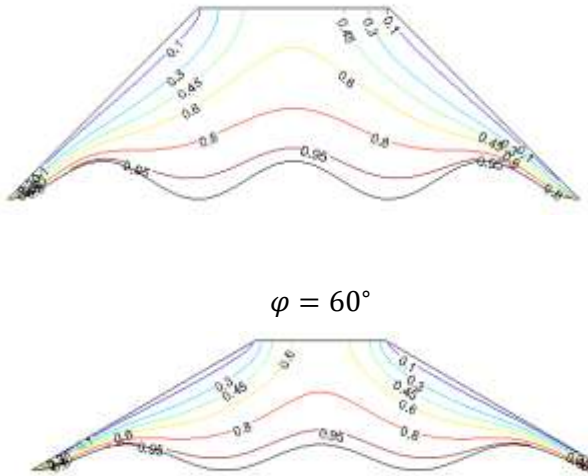

$\varphi = 60°$

Figure 4: Isotherm Plots for Different Values of φ with $Ec = 10^{-5}$ (Al_2O_3-Water Nanofluid)

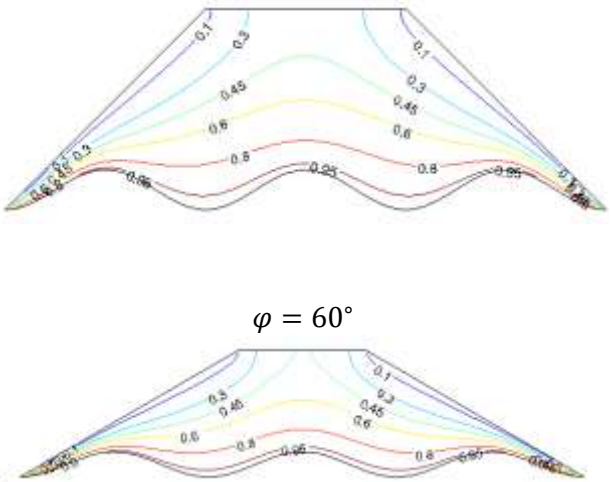

$\varphi = 60°$

Figure 5: Isotherm Plots for Different Values of φ with $Ec = 10^{-5}$ (SWCNT-Water Nanofluid)

Table 5: Average Nusselt Number for Different Values of $\boldsymbol{Ec}$ with $\boldsymbol{\varphi = 45°}$

Ec	Nu_{av} (Al_2O_3-Water Nanofluid)	Nu_{av} (SWCNT-Water Nanofluid)
10^{-6}	4.7524	5.0947
10^{-5}	4.7322	5.0947
10^{-4}	4.0716	5.0947

$Ec = 10^{-6}$

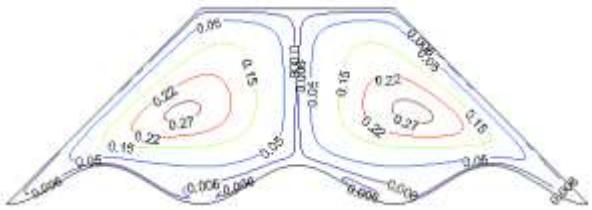

$Ec = 10^{-6}$

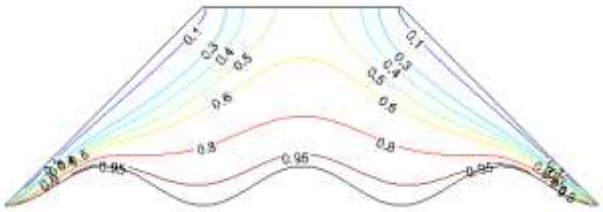

$Ec = 10^{-5}$

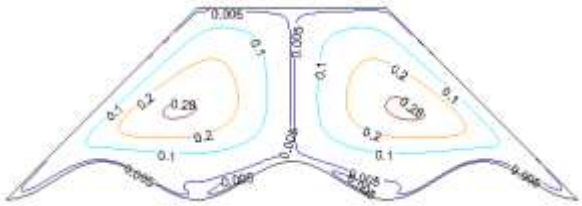

$Ec = 10^{-5}$

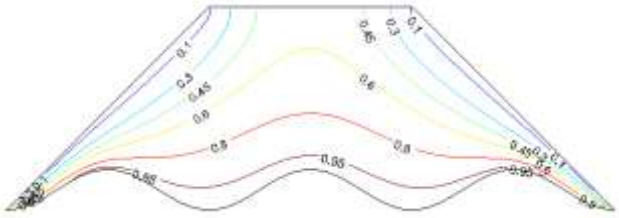

$Ec = 10^{-4}$

$Ec = 10^{-4}$

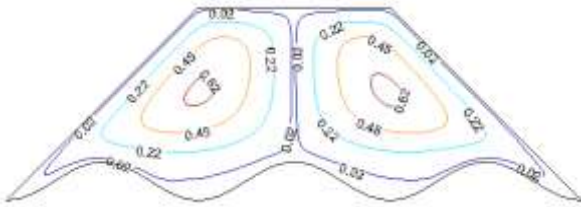

Figure 6: Streamline Plots for Different Values of Ec with $\varphi = 45°$ (Al_2O_3-Water Nanofluid)

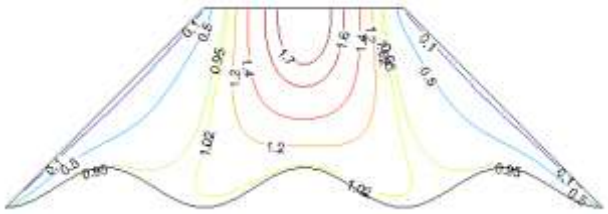

Figure 7: Isotherm Plots for Different Values of Ec with $\varphi = 45°$ (Al_2O_3-Water Nanofluid)

6. Conclusions

In this paper, the unsteady free convection flows of alumina-water and SWCNT-water nanofluids within a trapezoidal enclosure with corrugated bottom wall were considered. The influence of sidewall inclination angle φ and Eckert number Ec on fluid flow and heat transfer were discussed. The results showed that the flow circulation and fluid temperature increased as the side wall inclination angle increased. Furthermore, the heat transfer rate on the bottom wall was highest when the sidewall inclination angle was near $45°$. These findings are consistent with results obtained by Mamun et al. [9]. The velocity and temperature of the alumina-water nanofluid increased when the Eckert number was increased. Moreover, the rate of heat transfer was enhanced by reducing viscous and Joule dissipations.

References

[1] K. M. Khanafer, A. J. Chamkha. Mixed convection flow in a lid-driven enclosure filled with a fluid-saturated porous medium. *Int. J. Heat Mass Transfer* 42 no. 13, (1999) 2465-2481.
[2] A. J. Chamkha. Hydromagnetic combined convection flow in a vertical lid-driven cavity with internal heat generation or absorption. *Numerical Heat Transfer, Part A: Applications* 41, (2002) 529-546.
[3] M. Muthtamilselvan. Forced convection in a two-sided lid-driven cavity filled with volumetrically heat generating porous medium. *Int. J. of Appl. Math. and Mech.* 7 no. 13, (2011) 1-16.
[4] A. M. Karimipour, M. Afrand, M. Akbari, M. R. Safaei. Simulation of fluid flow and heat transfer in the inclined enclosure. *International Journal of Mechanical and Aerospace Engineering* 6, (2012) 86-91.
[5] W. Kalaoka, S. Witayangkurn. Natural convection in a porous square enclosure with partially cooled from vertical wall. *KMITL Sci. Tech. J.* 12 no. 2, (2012) 180-188.
[6] R. Roslan, H. Saleh, I. Hashim. Buoyancy-driven heat transfer in nanofluid-filled trapezoidal enclosure with variable thermal conductivity and viscosity. *Numerical Heat Transfer, Part A: Applications* 60, (2011) 867-882.
[7] S. M. Al-Weheibi, M. M. Rahman, M. S. Alam, K. Vajravelu. Numerical simulation of natural convection heat transfer in a trapezoidal enclosure filled with nanoparticles. *International Journal of Mechanical Sciences* 131-132, (2017) 599-612.
[8] W. Qu, G. M. Mala, D. Li. Heat transfer for water flow in trapezoidal silicon microchannels. *Int. J. Heat Mass Transfer* 43 no. 21, (2000) 3925-3936.
[9] M. A. H. Mamun, M. T. Islam, M. M. Rahman. Natural convection in a porous trapezoidal enclosure with magneto-hydrodynamic effect. *Nonlinear Analysis: Modelling and Control* 15 no. 2, (2010) 159-184.
[10] M. H. Esfe, A. A. A. Arani, W. Yan, H. Ehteram, A. Aghaie, M. Afrand. Natural convection in a trapezoidal enclosure filled with carbon nanotube-EG-water nanofluid. *Int. J. Heat Mass Transfer* 92, (2016) 76-82.
[11] P. Akbarzadeh, A. H. Fardi. Natural convection heat transfer in 2D and 3D trapezoidal enclosures filled with nanofluid. *Journal of Applied Mechanics and Technical Physics* 59 no. 2, (2018) 292-302.

[12] V. M. Job, S. R. Gunakala. Unsteady MHD free convection nanofluid flows within a wavy trapezoidal enclosure with viscous and Joule dissipation effects. *Numerical Heat Transfer, Part A: Applications* 69 no. 4, (2016) 421-443.
[13] V. M. Job, S. R. Gunakala, B. Rushi Kumar, R. Sivaraj. Time-dependent hydromagnetic free convection nanofluid flows within a wavy trapezoidal enclosure. *Applied Thermal Engineering* 11, (2017) 363-377.
[14] W. J. Minkowycz, E. M. Sparrow, J. P. Abraham. 2013. *Nanoparticle Heat Transfer and Fluid Flow, Vol. 4. of Advances in Numerical Heat Transfer*. CRC Press.
[15] J. Jiang, J. Wang, L. Baowen. Thermal expansion in single-walled carbon nanotubes and graphene: Nonequilibrium Green's function approach. *Physical Review B* 80, (2009) 205429.
[16] W. A. Khan, Z. H. Khan, M. Rahi. Fluid flow and heat transfer of carbon nanotubes along a flat plate with Navier slip boundary. *Appl. Nanosci.*, 4 no. 5, (2014) 633-641.
[17] Q. Li, Y. Li, X. Zhang, S. B. Chikkannanavar, Y. Zhao, A. M. Dangelewicz, L. Zheng, et al. Structure-dependent electrical properties of carbon nanotube fibers. *Advanced Materials* 19, (2007) 3358-3363.
[18] K. Sadoughi, M. Hosseini, F. Shakeri, M. Azimi. Analytical simulation of MHD nanofluid flow over the horizontal plate. *Frontiers in Aerospace Engineering* 2 no. 4, (2013) 242-246.
[19] C. R. Dohrmann, P. B. Bochev. A stabilized finite element method for the Stokes problem based on polynomial pressure projections. *International Journal for Numerical Methods in Fluids* 46 no. 2, (2004) 183-201.
[20] G. De Vahl Davis. Natural convection of air in a square cavity: a bench mark numerical solution. *International Journal for Numerical Methods in Fluids* 3, (1983) 249-264.